

MOL #68197

Title Page

**Effects of the allosteric antagonist PSNCBAM-1 on CB₁ receptor modulation in
the cerebellum**

Xiaowei Wang, James G. Horswill, Benjamin J. Whalley and Gary J. Stephens

School of Pharmacy University of Reading, Whiteknights, Reading, RG6 6AJ (X.W.,
B.J.W., G.J.S.); and Prosidion Limited, Windrush Court, Watlington Rd, Oxford, OX4
6LT (J.G.H.)

MOL #68197

Running Title Page

Running title: Ligand-dependent effects of PSNCBAM-1

Corresponding author:

Gary Stephens

School of Pharmacy

University of Reading

Whiteknights

PO Box 228

Reading RG6 6AJ

Tel: 44 118 378 6156

e-mail: g.j.stephens@reading.ac.uk

Abbreviations:

AM251: N-(piperidin-1-yl)-1-(2,4-dichlorophenyl)-5-(4-iodophenyl)-4-methyl-1H-multipyrazole-3-carboxamide; CP55950: (-)-cis-3-[2-hydroxy-4-(1,1-dimethyl heptyl)phenyl]-trans-4-(3-hydroxypropyl) cyclohexanol; PSNCBAM-1: 1-(4-chlorophenyl)-3-[3-(6-pyrrolidin-1-ylpyridin-2-yl)phenyl]urea; WIN55,212-2 (WIN55): R(+)-[2,3-dihydro-5-methyl-3-[(morpholinyl)methyl]-pyrrolo [1,2,3,-de]-1,4-benzoxazinyl]-(1-naphthalenyl) methanone mesylate

Number of text pages: 35

Number of tables: 0

Number of figures: 7 (and 1 Supplemental Figure)

MOL #68197

Number of references: 39

Number of words in the Abstract: 232

Number of words in the Introduction: 678

Number of words in the Discussion: 1546

MOL #68197

Abstract

PSNCBAM-1 has recently been described as a cannabinoid CB₁ receptor allosteric antagonist associated with hypophagic effects *in vivo*; however, PSNCBAM-1 effects on CB₁ ligand-mediated modulation of neuronal excitability remain unknown. Here, we investigate PSNCBAM-1 actions on CB₁ receptor-stimulated [³⁵S]GTPγS binding in cerebellar membranes and on CB₁ ligand modulation of presynaptic CB₁ receptors at inhibitory interneurone-Purkinje cell (IN-PC) synapses in the cerebellum using whole-cell electrophysiology. PSNCBAM-1 caused non-competitive antagonism in [³⁵S]GTPγS binding studies, with higher potency against the CB receptor agonist CP55940 than for WIN55,212-2 (WIN55). In electrophysiological studies, WIN55 and CP55940 reduced miniature inhibitory postsynaptic currents (mIPSCs) frequency, but not amplitude. PSNCBAM-1 application alone had no effect on mIPSCs; however, PSNCBAM-1 pre-treatment revealed agonist-dependent functional antagonism, abolishing CP55940-induced reductions in mIPSC frequency, but having no clear effect on WIN55 actions. The CB₁ antagonist/inverse agonist AM251 increased mIPSC frequency beyond control, this effect was reversed by PSNCBAM-1. PSNCBAM-1 pre-treatment also attenuated AM251 effects. Thus, PSNCBAM-1 reduced CB₁ receptor ligand functional efficacy in the cerebellum. The differential effect of PSNCBAM-1 on CP55940 versus WIN55 actions in [³⁵S]GTPγS binding and electrophysiological studies and the attenuation of AM251 effects are consistent with the ligand-dependency associated with allosteric modulation. These data provide the first description of functional PSNCBAM-1 allosteric antagonist effects on neuronal

MOL #68197

excitability in the mammalian CNS. PSNCBAM-1 allosteric antagonism may provide viable therapeutic alternatives to orthosteric CB₁ antagonists/inverse agonists in the treatment of CNS disease.

Introduction

Numerous G protein-coupled receptors (GPCRs) contain allosteric binding sites for endogenous and synthetic ligands that are topographically different from the orthosteric site (Christopoulos, 2002; Christopoulos and Kenakin, 2002; May and Christopoulos, 2003). On the basis of the ternary complex model, ligands at such allosteric sites mediate their cooperative effects on orthosteric affinity by altering rates of orthosteric ligand association and/or dissociation from the receptor (Ehlert, 1988; Christopoulos and Kenakin, 2002; May *et al.*, 2004; May *et al.*, 2007). Various therapeutic advantages of allosteric over orthosteric modulation have been suggested based on the differences between their underlying mechanisms (May and Christopoulos, 2003). In 2005, Price *et al.* identified three Organon compounds, Org 27659, Org 27759 and Org 29647 as allosteric modulators at CB₁ receptors, thereby revealing a CB₁ allosteric binding site that could hold potential as an alternative target for therapeutic modulation. More recently, Horswill *et al.* (2007) described the actions of a further novel CB₁ allosteric antagonist, 1-(4-chlorophenyl)-3-[3-(6-pyrrolidin-1-ylpyridin-2-yl) phenyl]urea (PSNCBAM-1). The Organon compounds and PSNCBAM-1 all showed ligand-dependent effects in that they increased agonist (-)-cis-3-[2-hydroxy-4-(1,1-dimethylheptyl)phenyl]- trans-4-(3-hydroxypropyl) cyclohexanol (CP55940) equilibrium binding, but decreased antagonist SR141716A (rimonabant) binding. Interestingly, and so-far unique to CB₁ receptors, allosteric modulation of orthosteric efficacy was in an opposite direction to effects on orthosteric binding affinity in these studies; thus, CB₁ allosteric antagonists produced

MOL #68197

non-competitive functional antagonism of CB₁ agonist effects (Ross, 2007a; 2007b). PSNCBAM-1 was also suggested to exhibit agonist-dependent actions on the basis that antagonism of human CB₁ stimulation by different agonists exhibited a wide range of potencies in a yeast reporter assay (Horswill *et al.*, 2007). Finally, CB₁ allosteric antagonism was proposed to be of functional relevance, as PSNCBAM-1 was also shown to possess hypophagic activity *in vivo* (Horswill *et al.*, 2007).

It has yet to be determined whether CB₁ allosteric antagonists influence functional CB₁-mediated modulation of neuronal excitability in the CNS. CB₁ receptors are prominently expressed on presynaptic terminals within the CNS where they are intimately involved in the dynamic modulation of transmitter release. Therefore, we have investigated PSNCBAM-1 modulation of effects of exogenous ligands on synaptic transmission at the well-characterized inhibitory pathway between molecular layer interneurons (IN) and Purkinje cells (PC). We and others have demonstrated that CB₁ receptor activation at IN-PC synapses reduces inhibitory neurotransmission (Llano *et al.*, 1991; Takahashi and Linden, 2000; Diana *et al.*, 2002; Diana and Marty, 2003; Kawamura *et al.*, 2006; Yamasaki *et al.*, 2006; Ma *et al.*, 2008; Kelm *et al.*, 2008). We have also previously combined patch-clamp and multi-electrode array electrophysiological recording techniques to show that CB₁ receptor ligand effects on inhibitory neurotransmission at IN-PC synapses functionally modulate cerebellar network activity (Ma *et al.*, 2008). In particular, CB₁ receptor antagonist action at IN-PC synapses is consistent with block on endocannabinoid tone to increase GABA release and reduce overall excitability in the

MOL #68197

cerebellum (Stephens, 2009). The recent clinical withdrawal of rimonabant, an agent shown to function as an inverse agonist at CB₁ receptors, has been linked to an inhibition of constitutive CB₁ activity, which can occur even in the absence of endocannabinoid release (Jones, 2008). Such potentially unfavourable actions could be avoided by use of neutral antagonists, which will only block the action of endocannabinoids released 'on demand'. However, a further attractive option is the development of allosteric CB₁ receptor antagonists to offer alternative therapeutic potential to orthosteric antagonists/inverse agonists (Ross, 2007a; 2007b). Moreover, since PC axons represent the sole efferent system from the cerebellar cortex, the present study provides an opportunity to determine whether CB₁ allosteric antagonists have potential to functionally modulate the output of the cerebellum.

Here, we show that PSNCBAM-1 causes an agonist-dependent functional antagonism of CB₁ receptor-mediated modulation of inhibitory neurotransmission at IN-PC synapses, consistent with the demonstration of non-competitive antagonism and agonist-dependent potency in [³⁵S]GTPγS binding studies in isolated cerebellar membranes. We extend data to PSNCBAM-1 effects to actions on the CB₁ receptor antagonist/inverse agonist N-(piperidin-1-yl)-1-(2,4-dichlorophenyl)-5-(4-iodophenyl)-4-methyl-1H-multipyrazole-3-carboxamide (AM251). The reduction in CB₁ receptor ligand-mediated functional efficacy in the cerebellum also extends previous studies demonstrating a unique response profile for CB₁ allosteric antagonists to actions on neuronal excitability.

Materials and methods

[³⁵S]GTPγS binding assays

Cerebellar membranes were prepared from C57Bl/6 mice and [³⁵S]GTPγS binding experiments performed as described previously (Horswell *et al.*, 2007; Dennis *et al.*, 2008). Briefly, 10 μg membranes per reaction were incubated with 10 μM GDP and 0.1 nM [³⁵S]GTPγS in assay buffer (20 mM HEPES, 3 mM MgCl₂, 100 mM NaCl, 1 mM DTT, 100 nM DPCPX, 1 mg/ml BSA; pH 7.4). DPCPX, an adenosine A₁ receptor antagonist, was included in the buffer to reduce non-CB₁ receptor-mediated [³⁵S]GTPγS binding. Reactions were performed in duplicate or triplicate in 96 well, round-bottom plates in a final volume of 200 μl; non-specific binding was determined using 10 μM unlabelled GTPγS. Antagonists were pre-incubated with membranes for 10 min at room temperature before adding agonists. After addition of agonists, plates were incubated for a further 15 min at room temperature (22-24°C) before adding [³⁵S]GTPγS. Plates were then incubated at 30°C for a further 45 min. Reactions were terminated by rapid filtration onto GF/B filter mats which were subsequently washed 5 times with 300 μl per well 50 mM Tris-HCl buffer (pH 7.4). Filter mats were dried and scintillation reagent added before counting radioactivity using a Perkin Elmer scintillation counter. PSNCBAM-1 effects were tested against a range of CB agonist concentrations. Dose-titration effects were also tested against a fixed agonist concentrations, as allowed by the non-competitive nature of antagonism; thus, CP55940 (150 nM) or R(+)-[2,3-dihydro-5-methyl-3-[(morpholinyl)methyl]-pyrrolo

MOL #68197

[1,2,3,-de]-1,4-benzoxazinyl)-(1-naphthalenyl) methanone mesylate (WIN55) (0.5 μ M) was used to stimulate [35 S]GTP γ S binding (to approximately 165% of basal) in the presence of a range of PSNCBAM-1 concentrations. Binding data were analysed using GraphPad Prism 5. Unpaired Student's *t*-tests were used to compare different agonist treatment values and pIC₅₀ values.

Electrophysiology

Preparation of acute cerebellar brain slices

3-5 week old male C57Bl/6 mice were used for all experiments, which followed methods outlined previously (Ma *et al.*, 2008). All work was conducted in accordance with UK Home Office regulations (Animals (Scientific Procedures) Act 1986) and every effort was made to minimize any discomfort experienced by animals. Mice were killed by cervical dislocation and decapitated. The brain was rapidly removed and submerged in ice-cold sucrose-based aCSF solution. The cerebellum was then hemisected along the midline and a hemisphere glued to the stage of a Vibratome (R and L Slaughter, Upminster, UK) that was used to prepare 300 μ m parasagittal cerebellar slices. After sectioning, each slice was immediately moved to a holding chamber containing standard aCSF, which consisted (in mM): NaCl 124, KCl 3, NaHCO₃ 26, NaH₂PO₄ 2.5, MgSO₄ 2, CaCl₂ 2, D-glucose 10; maintained at pH 7.3 by bubbling with 95% O₂/5% CO₂. Slices were kept at 37°C for at least 30 mins and then allowed to return to room temperature. Recordings were made 2-8 h after slice preparation. The sucrose-based aCSF solution used for dissection and slicing was

MOL #68197

identical to standard aCSF with the exception that NaCl was replaced by isosmotic sucrose.

Whole-cell patch clamp recording

Individual cerebellar brain slices were placed in a recording chamber maintained at room temperature and superfused with carboxygenated standard aCSF. PCs were identified using an IR-DIC upright Olympus BX50WI microscope (Olympus, Tokyo, Japan) with a 60x, 0.9 numerical aperture water immersion lens. Whole-cell patch clamp recordings were made from PCs at a holding potential of -70 mV using an EPC-9 amplifier (HEKA Elektronik, Lambrecht, Germany), controlled by Pulse software (HEKA) using a Macintosh G4 computer. Electrodes (3-7 M Ω) were pulled from borosilicate glass (GC150-F10, Harvard Apparatus, Kent, UK) filled with an intracellular solution containing (in mM): CsCl 140, MgCl₂ 1, CaCl₂ 1, EGTA 10, MgATP 4, NaGTP 0.4, HEPES 10; pH 7.3. For whole-cell recording, slow capacitance was compensated and series resistance typically monitored at 15-20 M Ω with 70-90% compensation. Data were sampled at 5 kHz and filtered at one-third of the sampling frequency. Spontaneous inhibitory postsynaptic currents were first recorded for a minimum of 15 mins to ensure recording stability. To isolate mIPSCs, slices were treated with tetrodotoxin (TTX, 1 μ M) and NBQX (2.5 μ M). In all experiments, ligands were bath applied for a minimum of 20 minutes to achieve maximal steady-state effects and a minimum 150 s recording was used as raw data for event detection. Solvent was present at a maximum final concentration of 0.1% v/v;

MOL #68197

solvent, applied alone at equivalent experimental concentrations, has no effect on synaptic responses in this preparation (Bardo *et al.*, 2002).

Data and statistical analysis

Data were initially exported using Pulsefit (HEKA) and then imported to AxoGraph 4.0 software for event detection. All electrophysiology data were analyzed using GraphPad Prism 4 or Axograph 4.0 software. Cumulative frequency plots were constructed for inter-event intervals using 5 ms bins. In the all cases, since amplitude distributions were skewed and did not pass the D'Agostino and Pearson omnibus normality test, differences between the means of the medians were used for parametric testing. Cumulative frequency plots were analyzed using the Kolmogorov-Smirnov test. Paired Student's *t*-tests were used to compare control and first treatment values. Comparison of the means from multiple treatment groups was performed using repeated measurement one-way ANOVA tests. Tukey's HSD tests were performed when a repeated measurement one-way ANOVA yielded significant differences. Differences were considered significant if $p < 0.05$. All data are expressed as means \pm SEM; n refers to the number of replicants used.

Pharmacology

The following agents were used: AM251, CP55940, NBQX (disodium salt), WIN55 (all Tocris Cookson, Bristol, UK), (R)-baclofen (Ascent Scientific, Bristol, UK) and TTX-citrate (Alomone Labs, Jerusalem, Israel). PSNCBAM-1 was kindly provided by

MOL #68197

Prosidion Limited. TTX-citrate was dissolved in distilled water and NBQX, WIN55, PSNCBAM-1 and AM251 were dissolved in DMSO. All drugs were made up as 1000x stock solutions except AM251 (made up as 5000x stock) and stored at -20°C. Drug stock solutions were diluted in carboxygenated standard aCSF immediately before application.

Results

Previous studies have identified PSNCBAM-1 as an allosteric antagonist at recombinant human CB₁ receptors (Horswill *et al.* 2007). We first sought to extend studies to CB₁ receptors in native murine cerebellar membranes (Dennis *et al.*, 2008). The CB receptor agonist CP55940 stimulated [³⁵S]GTPγS binding to a maximum of 172.0 ± 7.3% of basal (n=4) with a pEC₅₀ of 8.04 ± 0.03 (Fig. 1A). The CB receptor agonist WIN55 also stimulated [³⁵S]GTPγS binding, but with a significantly higher maximum effect (236.5 ± 6.2% of basal, n=4, p<0.01, Student's *t*-test) and a significantly less potent pEC₅₀ of 6.22 ± 0.10 (p<0.01, Student's *t*-test) than seen for CP55940 (Fig. 1B). PSNCBAM-1 behaved non-competitively against both CB receptor agonists, producing a substantial reduction in maximal [³⁵S]GTPγS stimulation, whilst only weakly affecting agonist potency. Agonist-dependent effects were also seen; for example, 1 μM PSNCBAM-1 was sufficient to almost fully inhibit CP55940 stimulation, by contrast, 10 μM PSNCBAM-1 was unable to fully inhibit the WIN55-induced response. We further investigated this phenomenon by determining PSNCBAM-1 potency for inhibition against a single agonist concentration that stimulated a similar amount of GTPγS binding. Whilst these experiments are dependent on the agonist concentration chosen, PSNCBAM-1 displayed significantly greater potency against CP55940 than WIN55 (pIC₅₀ of 7.32 ± 0.20 and 6.50 ± 0.15 respectively, p<0.05, Student's *t*-test). Overall, these data confirm PSNCBAM-1 non-competitive, agonist-dependent actions in [³⁵S]GTPγS binding assays.

Effects of PSNCBAM-1 on CB receptor agonist modulation of inhibitory neurotransmission.

Having demonstrated that PSNCBAM-1 has differential agonist-dependent actions in [³⁵S]GTPγS binding assays in isolated cerebellar membranes, we next examined the potential functional effects of PSNCBAM-1 on modulation of synaptic transmission at IN-PC synapses in C57Bl/6 mice. We first confirmed that WIN55 exerted a comparable agonistic effect to that previously demonstrated in TO strain mice (Ma *et al.*, 2008). Bath application of WIN55 (5 μM) significantly decreased mean mIPSC frequency (73 ± 6%, n=8, p<0.01, Student's *t*-test; Fig. 2A), there was no accompanying change in mean mIPSC amplitude (n=8; p=0.52, Student's *t*-test). CP55940 (5 μM) also significantly decreased mean mIPSC frequency (64 ± 6%, n= 6, p<0.01, Student's *t*-test; Fig. 2B), again, with no effect on amplitude distribution (n=6; p=0.99, Student's *t*-test). In these and all subsequent experiments, no statistically significant changes in mean mIPSC amplitude were seen and these effects are not further discussed. Overall, these data are consistent with a reduction in presynaptic GABA release without accompanying postsynaptic changes and so confirm CB₁ agonist effects at IN-PC synapses (Ma *et al.*, 2008) to be independent of the mouse strain used.

To examine effects of PSNCBAM-1 upon CB₁ agonist-mediated modulation of inhibitory transmission in the cerebellum, WIN55 or CP55940 was applied in the presence of PSNCBAM-1 (Fig. 3). Pre-treatment with 10 μM PSNCBAM-1 had no significant effect on WIN55-induced inhibition of synaptic transmission, such that 5

MOL #68197

μM WIN55 still caused a significant decrease in mean mIPSC frequency ($76 \pm 4\%$, $n=7$, $p<0.01$, Student's *t*-test; Fig. 3A). By marked contrast, PSNCBAM-1 abolished the inhibitory effect of $5 \mu\text{M}$ CP55940 on mean mIPSC frequency ($97 \pm 11\%$, $n=5$, $p=0.83$, Student's *t*-test; Fig. 3B). Together, these data demonstrate PSNCBAM-1 can cause CB receptor functional antagonism at IN-PC synapses and reflect an agonist-dependent effect.

Effects of PSNCBAM-1 on CB₁ receptor antagonist modulation of inhibitory neurotransmission.

In our previous study, we reported that the synthetic CB₁ antagonist/inverse agonist AM251 increased inhibitory neurotransmission at IN-PC synapses in TO strain mice, as demonstrated by an increase in mean mIPSC frequency beyond control levels (Ma *et al.*, 2008). This increase can be generally attributable to the removal of endocannabinergic tone by a CB₁ antagonist action or the blockade of constitutive activity by an inverse agonist action. Therefore, we next compared the actions of PSNCBAM-1 with those of AM251 at IN-PC synapses in C57Bl/6 mice. $10 \mu\text{M}$ PSNCBAM-1 had no significant effect on mean mIPSC frequency ($99 \pm 6\%$, $n=12$, $p=0.80$, Student's *t*-test; Fig. 4A). By contrast, $2 \mu\text{M}$ AM251 caused a significant increase in mean mIPSC frequency ($117 \pm 4\%$, $n=7$, $p<0.01$, Student's *t*-test; Fig. 4B). These data suggest that PSNCBAM-1 lacks the CB₁ neutral antagonist or inverse agonist properties associated with AM251 in this system.

To confirm these data, next we activated CB receptors with WIN55 before

MOL #68197

application of either AM251 or PSNCBAM-1 (Fig. 5). In the first of these experiments, 5 μM WIN55 caused a significant reduction in mean mIPSC frequency ($74 \pm 4\%$, $p < 0.01$, Student's *t*-test) which was reversed to beyond control level by subsequent application of 2 μM AM251 ($115 \pm 7\%$, $n=7$, $p < 0.001$, repeated measurement one-way ANOVA followed by a Tukey's HSD test; Fig. 5A). By contrast, in a separate set of experiments, the 5 μM WIN55-induced significant reduction in mean mIPSC frequency ($74 \pm 6\%$, $p < 0.01$, Student's *t*-test) was not significantly affected by 10 μM PSNCBAM-1 ($71 \pm 8\%$, $n=8$, $p > 0.05$, repeated measurement one-way ANOVA followed by a Tukey's HSD test; Fig. 5B). Subsequent application of AM251 was still able to reverse WIN55 effects (mean mIPSC frequency increased to $97 \pm 6\%$, $n=8$; $p < 0.01$, repeated measurement one-way ANOVA followed by a Tukey's HSD test; Fig. 5B). In this experiment, mean mIPSC frequency in the presence of AM251 did not exceed control levels, suggesting that PSNCBAM-1 pre-treatment can affect AM251 actions; therefore, we next examined the effects of PSNCBAM-1 application after AM251 (Fig. 6). In this set of experiments, 2 μM AM251 caused a significant increase in mean mIPSC frequency ($117 \pm 4\%$, $n=7$; $p < 0.01$, repeated measurement one-way ANOVA followed by a Tukey's HSD test) which, in turn, was significantly reduced by subsequent application of 10 μM PSNCBAM-1 ($104 \pm 3\%$, $n=7$; $p < 0.01$, repeated measurement one-way ANOVA followed by a Tukey's HSD test; Fig. 6). These data demonstrate that PSNCBAM-1 had actions on a CB_1 antagonist/inverse agonist in addition to the agonist-dependent modulation described above.

Finally, to test for potential actions at other $\text{G}\alpha_{i/o}$ -coupled GPCRs that modulate

MOL #68197

inhibitory transmission at IN-PC synapses, we investigated PSNCBAM-1 effects on GABA_B receptor-mediated inhibition (Harvey and Stephens, 2004). Bath application of the GABA_B agonist baclofen (20 μM) significantly decreased mean mIPSC frequency ($78 \pm 3\%$, $n=4$, $p<0.01$, Student's *t*-test; Fig. 7A). Pre-treatment with 10 μM PSNCBAM-1 had no significant effect on baclofen-induced inhibition of synaptic transmission, such that 20 μM baclofen still caused a significant decrease in mean mIPSC frequency ($72 \pm 4\%$, $n= 5$, $p<0.01$, Student's *t*-test; Fig. 7B).

Taken together, these electrophysiological data suggest that PSNCBAM-1 displays CB₁ receptor ligand-dependent actions consistent with functional allosteric antagonism at cerebellar IN-PC synapses.

Discussion

Recent studies have identified a series of Organon compounds and the structurally similar PSNCBAM-1 as CB₁ receptor allosteric antagonists (Price *et al.*, 2005; Horswill *et al.* 2007). Here, we demonstrate PSNCBAM-1 functional CB₁ antagonism and agonist-dependent effects on [³⁵S]GTPγS binding in native cerebellar membranes and reveal that these effects extend to CB₁ ligand-dependent modulation of inhibitory neurotransmission in the mammalian CNS.

PSNCBAM-1 displays agonist-dependent potency in [³⁵S]GTPγS binding assays

PSNCBAM-1 caused a non-competitive antagonism of CB receptor agonist-stimulated [³⁵S]GTPγS binding in cerebellar membranes. Overall, PSNCBAM-1 achieved only a partial inhibition of WIN55-induced responses, with PSNCBAM-1 displaying higher potency for inhibition of CP55940 *versus* WIN55 stimulation when tested against a range of agonist concentration and in dose-titration experiments against a fixed agonist concentration. A similar differentiation was seen in HEK293 membranes expressing the human CB₁ receptor, where PSNCBAM-1 also displayed higher potency for inhibition of agonist-stimulated [³⁵S]GTPγS binding by CP55940 than by WIN55 (Supplemental data Fig. 1). Thus, PSNCBAM-1 displays agonist-dependent potency at mouse CB₁ receptors in native membranes and recombinant human CB₁ receptors. A caveat to these data is that WIN55 may stimulate a non-CB₁-mediated component of [³⁵S]GTPγS binding (Breivogel *et al.*, 2001). In the present study, WIN55 displayed a higher efficacy than CP55940 in

MOL #68197

stimulation of [³⁵S]GTPγS binding in cerebellar membranes, as reported in some previous studies (Breivogel *et al*, 2003; Childers, 2006). However, we have shown that WIN55-stimulated [³⁵S]GTPγS binding in cerebellar membranes is potently blocked by the CB₁ antagonists AM251 and Δ⁹-tetrahydrocannabivarin (Δ⁹-THCV) (Dennis *et al.*, 2008), and that WIN55 inhibition at IN-PC synapses is prevented by Δ⁹-THCV (Ma *et al.*, 2008), arguing against WIN55 causing *functional* CB₁-independent effects here. With regard to alternative receptor targets, it is of interest that CP55940, but not WIN55, is a ligand at GPR55, an lysophosphatidylinositol receptor, with some sensitivity to cannabinoids (Ross, 2009). However, in our hands, the GPR55 agonist O-1602 lacked effects on [³⁵S]GTPγS binding in cerebellar membranes (Smith, Whalley and Stephens, unpublished data). Moreover, it is currently unknown if PSNCBAM-1 acts at GPR55. In the future, it will be useful to test effects of CB₁ allosteric antagonists in *cnr1*^{-/-} and *GPR55*^{-/-} animals. Overall, PSNCBAM-1 displays both non-competitive antagonism and agonist-dependent potency in [³⁵S]GTPγS binding studies, characteristics associated with allosteric mechanisms (Conn *et al*, 2009).

C57Bl/6 mouse IN-PC synapses possess functional CB₁ receptors

Activation of CB₁ receptors at IN-PC synapses attenuates inhibitory neurotransmission, resulting in consequential synaptic disinhibition of PC output (Ma *et al.*, 2008). Here, both WIN55 and CP55940 caused a significant decrease in mIPSC frequency, but produced no change in mIPSC amplitude, consistent with CB₁

MOL #68197

agonist-mediated presynaptic inhibition of GABA release. We choose to record mIPSCs not only to isolate presynaptic events, but also to negate any potentially confounding WIN55-mediated effect on Ca^{2+} channels, which has been proposed to underlie WIN55 CB_1 receptor-independent effects on synaptic transmission (Nemeth *et al.*, 2008) and postsynaptic PC output (Fisyunov *et al.*, 2006). Since miniature, action potential-independent events at IN-PC synapses occur independently of Ca^{2+} influx into the axon terminal via voltage-dependent Ca^{2+} channels (Harvey and Stephens, 2004; Stephens, 2009), it is unlikely that such a mechanism could account for the observed WIN55-induced reduction in inhibitory transmission. Consequently, we propose that the CB_1 pathway mediating responses seen here occurs downstream of Ca^{2+} entry, involves the release machinery and results in the inhibition of exocytosis of GABA-containing vesicles. We also demonstrate that AM251 increases inhibitory neurotransmission. Together, these results confirm functional presynaptic CB_1 receptors at IN-PC synapses in C57Bl/6 mice, thereby validating the preparation for the study of functional PSNCBAM-1 effects.

PSNCBAM-1 displays agonist-dependent potency in electrophysiological studies

PSNCBAM-1 pre-treatment blocked CP55940-induced inhibition of synaptic transmission, by contrast, PSNCBAM-1 had no effect upon WIN55-induced inhibition. Thus, PSNCBAM-1 possesses an agonist-dependent functional antagonism at IN-PC synapses. This agonist-dependency is in agreement with our [^{35}S]GTP γ S binding assays and data from yeast reporter assays by Horswill *et al.* (2007) that

MOL #68197

showed PSNCBAM-1 more potently antagonized the stimulation of CB₁ receptors by CP55940 than by WIN55.

Here, PSNCBAM-1 had no effect on inhibitory neurotransmission when applied alone; by contrast, the CB₁ antagonist/inverse agonist AM251 increased mIPSC frequency. We have previously shown that AM251, Δ⁹-THCV and SR141716A all increase inhibitory neurotransmission at IN-PC synapses, an effect consistent with a blockade of endocannabinergic tone or abolition of constitutive CB₁ activity (Ma *et al.*, 2008). Moreover, pharmacological actions of PSNCBAM-1 exhibit assay-dependency, behaving as a non-competitive antagonist in an *in vivo* feeding model and CB₁ yeast reporter, GTPγS and cAMP assays, but demonstrating partial inverse agonism against basal [³⁵S]GTPγS binding (Horswill *et al.* 2007). Here, PSNCBAM-1 lacked the intrinsic activity associated with CB₁ antagonists/inverse agonists at IN-PC synapses. We have proposed that AM251 acts to displace endocannabinoids at IN-PC synapses (Stephens, 2009), the lack of intrinsic PSNCBAM-1 effects further suggests that PSNCBAM-1 binds at a site distinct from that occupied by endocannabinoids. Interestingly, PSNCBAM-1 modulated the actions of AM251. Thus, PSNCBAM-1 attenuated the AM251-induced reversal of WIN55-induced inhibition and also reversed AM251-induced increases in inhibitory neurotransmission. These data are the first to describe PSNCBAM-1 functional effects on CB₁ antagonists/inverse agonists and suggest further mechanisms of CB₁ receptor allosteric modulation.

MOL #68197

Mechanisms of PSNCBAM-1 allosteric antagonism

We demonstrate that PSNCBAM-1 has distinct effects on the actions of the CB agonist CP55940 *versus* WIN55 and also modulates the actions of the CB₁ antagonist/inverse agonist AM251. A parsimonious explanation of our data is that PSNCBAM-1 can bind to a CB₁ receptor allosteric site to exert a ligand-dependent antagonist action. Here, allosteric-orthosteric ligand interactions could also be dependent on the presence of different CB₁ orthosteric binding sites for distinct ligands. In this regard, molecular modelling studies have shown that CP55940 (a synthetic derivative of Δ^9 -tetrahydrocannabinol (Δ^9 -THC) and WIN55 (an aminoalkylindole) bind at distinct CB₁ binding sites (McAllister *et al.*, 2003; 2004), in agreement with earlier mutagenesis studies (Song and Bonner, 1996). Thus, PSNCBAM-1 allosteric binding may selectively affect different CB₁ orthosteric sites. The phenomenon whereby certain allosteric agents can interact with one class of ligands, but not another, has been termed ‘probe-dependence’ and is likely to be conserved across GPCR classes (Leach *et al.*, 2007; May *et al.*, 2007; Kenakin, 2008). In the classical ternary complex model for receptor allostery (Ehlert *et al.*, 1988), binding to an allosteric site alters ligand affinity for the orthosteric site in either a positive, negative or neutral direction. PSNCBAM-1 had positive cooperativity for agonist [³H]CP55940 binding, but negative cooperativity for antagonist/inverse agonist [³H]SR141716A binding in competition experiments (Horswill *et al.*, 2007). Comparable effects were reported for Organon CB₁ allosteric antagonists (Price *et al.*, 2005). Thus, CB₁ allosteric antagonists exhibit ligand-dependent actions on orthosteric affinity (Ross, 2007a;

MOL #68197

2007b). Moreover, in a manner that is presently unique to CB₁ allosteric antagonists, changes in orthosteric efficacy are reported to occur in an opposite direction to those on orthosteric affinity, with these compounds causing non-competitive antagonism of CB₁ receptor function. It may be hypothesized that interference with G proteins or G protein coupling may explain why CB₁ allosteric antagonists enhance CP55940 receptor binding, but inhibit CP55940 functional effects. However, it has previously been reported that PSNCBAM-1 lacks effects on CB₂ receptors, the closest homologue to CB₁ (Horswill *et al.*, 2007), and here we demonstrate that PSNCBAM-1 lacked modulatory effects on GABA_B receptor pathways at IN-PC synapses. Together with the differential effects on CB₁ ligands, these data suggest a lack of ‘non-selective’ PSNCBAM-1 actions on G proteins or their coupling.

Overall, our data is consistent with PSNCBAM-1 binding to a CB₁ receptor allosteric site leading to a reduction of receptor function efficacy for both CP55940 and AM251. These data extend demonstrations of reduced receptor function by CB₁ allosteric antagonists to functional assays of neuronal excitability and show that PSNCBAM-1 differentially affects CB₁ ligand-mediated modulation of inhibitory neurotransmission.

Therapeutic potential of CB₁ allosteric antagonists

CB₁ receptor activation by exogenous agents (e.g. Δ^9 -THC) results in severe motor incoordination and associated cerebellar dysfunction (DeSanty and Dar, 2001; Patel and Hillard, 2001). Therefore, blockade of CB₁ receptors could offer a viable

MOL #68197

therapeutic strategy in diseases such as cerebellar ataxia. A variety of therapeutic advantages of GPCR allosteric modulators have been described. Firstly, GPCR allosteric binding sites show divergence (Christopoulos, 2002), which could be exploited to reduce side-effects (Jensen and Spalding, 2004). Secondly, allosteric modulators may produce effects irrespective of dose, reducing the potential for toxicity (May and Christopoulos, 2003). For example, no adverse or toxic effects were seen following chronic PSNCBAM-1 administration *in vivo* (Horswill *et al.*, 2007). Finally, allosteric antagonists can lack intrinsic effects in the absence of an orthosteric ligand, allowing selective tuning of drug effects (Birdsall *et al.*, 1996; Christopoulos and Kenakin, 2002). Here, PSNCBAM-1 lacked intrinsic activity at IN-PC synapses; by contrast, CB₁ antagonists/inverse agonists increase inhibitory transmission (see also Ma *et al.* 2008). Intrinsic changes to neuronal excitability may be undesirable; for example, the withdrawal of rimonabant as an anti-obesity agent was proposed to reflect constitutive CB₁ activation due to inverse agonist actions (Jones, 2008). Thus, PSNCBAM-1 acting at an allosteric binding site has potential to reduce CNS side-effects associated with orthosteric CB₁ antagonist/inverse agonists.

Overall, we demonstrate PSNCBAM-1 actions consistent with non-competitive, agonist-dependent allosteric antagonism of cerebellar CB₁ receptors. These data extend PSNCBAM-1 functional effects to CB₁ ligand modulation of inhibitory neurotransmission and suggest alternative pharmacological approaches to the therapeutic modulation of neuronal excitability in the CNS.

MOL #68197

Acknowledgements

Thanks to Prosidion Ltd for supply of PSNCBAM-1. Work funded by an Ataxia UK Studentship awarded to BJW and GJS and supporting XW; XW also supported by a University of Reading International Postgraduate Research Studentship.

Authorship Contributions

Participated in research design: Wang, Horswill, Whalley and Stephens.

Conducted experiments: Wang and Horswill.

Contributed new reagents or analytic tools: Horswill.

Performed data analysis: Wang and Horswill.

Wrote or contributed to the writing of the manuscript: Wang, Horswill, Whalley and Stephens.

Other: Whalley and Stephens acquired funding for the research.

MOL #68197

References

Bardo S, Robertson B and Stephens GJ (2002) Presynaptic internal Ca^{2+} stores contribute to inhibitory neurotransmitter release onto mouse cerebellar Purkinje cells.

Br J Pharmacol **137**: 529-537.

Birdsall NJ, Lazareno S and Matsui H (1996) Allosteric regulation of muscarinic receptors. *Prog Brain Res* **109**: 147-151.

Breivogel CS, Griffin G, Di Marzo V and Martin BR (2001) Evidence for a new G protein-coupled cannabinoid receptor in mouse brain. *Mol Pharmacol* **60**: 155-163.

Breivogel CS, Scates SM, Beletskaya IO, Lowery OB, Aceto MD and Martin BR (2003) The effects of Δ^9 -tetrahydrocannabinol physical dependence on brain cannabinoid receptor. *Eur J Pharmacol* **459**: 139-150.

Childers SR (2006). Activation of G-proteins in brain by endogenous and exogenous cannabinoids. *AAPS Journal* **8**: E112-E117.

Christopoulos A (2002) Allosteric binding sites on cell-surface receptors: novel targets for drug discovery. *Nat Rev Drug Discov* **1**: 198-210.

Christopoulos A and Kenakin T (2002) G protein-coupled receptor allosterism and

MOL #68197

complexing. *Pharmacol Rev* **54**: 323–374.

Conn PJ, Christopoulos A and Lindsley CW (2009) Allosteric modulators of GPCRs: a novel approach to CNS disorders. *Nat Rev Drug Discov* **8**: 41-54.

Dennis I, Whalley BJ and Stephens GJ (2008) Effects of Δ^9 -tetrahydrocannabivarin on [35 S]GTP γ S binding in mouse brain cerebellum and piriform cortex membranes. *Br J Pharmacol* **154**: 1349-1359.

DeSanty KP and Dar MS (2001) Cannabinoid-induced motor incoordination through the cerebellar CB₁ receptor in mice. *Pharmacol Biochem Behav* **69**: 251–259.

Diana MA, Levenes C, Mackie K and Marty A (2002) Short-term retrograde inhibition of GABAergic synaptic currents in rat Purkinje cells is mediated by endogenous cannabinoids. *J Neurosci* **22**: 200–208.

Diana MA and Marty A (2003) Characterization of depolarization-induced suppression of inhibition using paired interneuron-Purkinje cell recordings. *J Neurosci* **23**: 5906-5918.

Ehlert FJ (1988) Estimation of the affinities of allosteric ligands using radioligand binding and pharmacological null methods. *Mol Pharmacol* **33**: 187–194.

MOL #68197

Fisyunov A, Tsintsadze V, Min R, Burnashew N and Lozovaya N (2006)

Cannabinoids modulate the P-type high-voltage-activated calcium currents in Purkinje neurons. *J Neurophysiol* **96**: 1267-1277.

Harvey VL and Stephens GJ (2004) Mechanism of GABA_B receptor-mediated inhibition of spontaneous GABA release onto cerebellar Purkinje cells. *Eur J Neurosci* **20**: 684-690.

Horswill JG, Bali U, Shaaban S, Keily JF, Jeevaratnam P, Babbs AJ, Reynet C and Wong Kai In P (2007) PSNCBAM-1, a novel allosteric antagonist at cannabinoid CB₁ receptors with hypophagic effects in rats. *Br J Pharmacol* **152**: 805-814.

Jensen AA and Spalding TA (2004) Allosteric modulation of G-protein coupled receptors. *Eur J Pharm Sci* **21**: 407-420.

Jones D (2008) End of the line for cannabinoid receptor 1 as an anti-obesity target. *Nat Rev Drug Discov* **7** **12**: 961-962.

Kawamura Y, Fukaya M, Naejima T, Yoshida T, Miura E, Watanabe M, Ohno-Shosaku T and Kano M (2006) CB₁ is the major cannabinoid receptor at excitatory presynaptic site in the hippocampus and cerebellum. *J Neurosci* **26**:

MOL #68197

2991–3001.

Kelm MK, Criswell HE and Breese GR (2008) The role of protein kinase A in the ethanol-induced increase in spontaneous GABA release onto cerebellar Purkinje neurons. *J Neurophysiol* **100**: 3417-3428.

Kenakin T (2008) Functional selectivity in GPCR modulator screening. *Comb Chem High Throughput Screen* **11**: 337-343.

Leach K, Sexton PM and Christopoulos A (2007) Allosteric GPCR modulators: taking advantage of permissive receptor pharmacology. *Trends Pharmacol Sci* **28**: 382-389.

Llano I, Leresche N and Marty A (1991) Calcium entry increase the sensitivity of cerebellar Purkinje cells to applied GABA and decrease inhibitory synaptic currents. *Neuron* **6**: 565-574.

Ma YL, Weston SE, Whalley BJ and Stephens GJ (2008) The phytocannabinoid Δ^9 -tetrahydrocannabivarin modulates inhibitory neurotransmission in the cerebellum. *Br J Pharmacol* **154**: 204-215.

May LT, Avlani VA, Sexton PM and Christopoulos A (2004) Allosteric modulation of G protein-coupled receptors. *Curr Pharm Des* **10**: 2003-2013.

MOL #68197

May LT and Christopoulos A (2003) Allosteric modulators of G-protein-coupled receptors. *Curr Opin Pharmacol* **5**: 551-556.

May LT, Leach K, Sexton PM and Christopoulos A (2007) Allosteric modulation of G protein-coupled receptors. *Annu Rev Pharmacol Toxicol* **47**: 1-51.

McAllister SD, Hurst DP, Barnett-Norris J, Lynch D, Reggio PH and Abood ME (2004) Structural mimicry in class A G protein-coupled receptor rotamer toggle switches: the importance of the F3.36(201)/W6.48(357) interaction in cannabinoid CB₁ receptor activation. *J Biol Chem* **279**: 48024-48037.

McAllister SD, Rizvi G, Anavi-Goffer S, Hurst DP, Barnett-Norris J, Lynch D, Reggio PH and Abood ME (2003) An aromatic microdomain at the cannabinoid CB₁ receptor constitutes an agonist/inverse agonist binding region. *J Med Chem* **46**: 5139-5152.

Németh B, Ledent C, Freund TF and Hájos N (2008) CB₁ receptor-dependent and -independent inhibition of excitatory postsynaptic currents in the hippocampus by WIN 55,212-2. *Neuropharmacol* **54**: 51-57.

Patel S and Hillard CJ (2001) Cannabinoid CB₁ receptor agonists produce cerebellar dysfunction in mice. *J Pharmacol Exp Ther* **297**: 629-637.

Price MR, Baillie GL, Thomas A, Stevenson LA, Easson M, Goodwin R, McLean A,

MOL #68197

McIntosh L, Goodwin G, Walker G, Westwood P, Marrs J, Thomson F, Cowley P,

Christopoulos A, Pertwee RG and Ross RA (2005) Allosteric modulation of the cannabinoid CB₁ receptor. *Mol Pharmacol* **68**: 1485–1495.

Ross RA (2007a) Allosterism and cannabinoid CB₁ receptors: the shape of things to come. *Trends Pharmacol Sci* **28**: 567-572.

Ross RA (2007b) Tuning the endocannabinoid system: allosteric modulators of the CB₁ receptor. *Br J Pharmacol* **152**: 565-566.

Ross RA (2009) The enigmatic pharmacology of GPR55. *Trends Pharmacol Sci* **30**: 156-163.

Song ZH and Bonner TI (1996) A lysine residue of the cannabinoid receptor is critical for receptor recognition by several agonists but not WIN55212-2. *Mol Pharmacol* **49**: 891-896.

Stephens GJ (2009) G-protein-coupled-receptor-mediated presynaptic inhibition in the cerebellum. *Trends Pharmacol Sci* **30**: 421-430.

Takahashi KA and Linden DJ (2000) Cannabinoid receptor modulation of synapses received by cerebellar Purkinje cells. *J Neurophysiol* **83**: 1167–1180.

Yamasaki M, Hashimoto K and Kano M (2006) Miniature synaptic events elicited by

MOL #68197

presynaptic Ca^{2+} rise are selectively suppressed by cannabinoid receptor activation in cerebellar Purkinje cells. *J Neurosci* **26**: 86–95.

Legends for Figures

Figure 1. Effects of PSNCBAM-1 on [³⁵S]GTPγS binding in mouse cerebellar membranes

Effects of PSNCBAM-1 on log concentration-response curves for A) CP55940 B) WIN55 on percentage basal stimulation of [³⁵S]GTPγS binding (both mean ± SEM of 4 experiments). C) Dose-titration effect of PSNCBAM-1 on either CP55940 (150 nM) or WIN55 (0.5 μM) stimulated [³⁵S]GTPγS binding in mouse cerebellar membranes. Data points are mean ± SEM of 3 experiments. PSNCBAM-1 had agonist-dependent potency differences between CP55940 (pIC₅₀ = 7.32 ± 0.20) versus WIN55 (pIC₅₀ = 6.50 ± 0.15); p<0.05, Student's *t*-test.

Figure 2. Effects of CB agonists on inhibitory neurotransmission at IN-PC synapses.

Effect of A) 5 μM WIN55 (n=8) and B) 5 μM CP55940 (n=6) on mIPSCs; (upper panel) example raw data traces, (middle panel) summary bar graph showing effects on normalized mIPSC frequency, (lower panel) cumulative frequency curves for effects on inter-event interval. Both WIN55 and CP55940 significantly reduced normalised mIPSC frequency (*p<0.01 *versus* control (CTL), Student's *t*-test) and caused a significant rightward shift of the CTL inter-event interval curve (both p<0.0001 in individual cells, Kolmogorov-Smirnov test).

MOL #68197

Figure 3. Effect of pre-treatment with PSNCBAM-1 on CB agonists

Effect of 10 μ M PSNCBAM-1 on A) 5 μ M WIN55 (n=7) and B) 5 μ M CP55940 (n=5) actions on mIPSCs; (upper panel) example raw data traces, (middle panel) summary bar graph showing effects on normalized mIPSC frequency, (lower panel) cumulative frequency curves for effects on inter-event interval. PSNCBAM-1 had agonist-dependent potency differences, blocking CP55940 effects, but lacking action on WIN55 effects, such that the WIN55-mediated significant reduction in normalised mIPSC frequency (* $p < 0.01$ versus control (CTL), Student's *t*-test) and significant rightward shift of the CTL inter-event interval curve ($p < 0.0001$ in individual cells, Kolmogorov-Smirnov test) were sustained.

Figure 4. Effect of PSNCBAM-1 and AM251 on inhibitory neurotransmission at IN-PC synapses.

Effect of A) 10 μ M PSNCBAM-1 (n=12) and B) 2 μ M AM251 (n=7) on mIPSCs; (upper panel) example raw data traces, (middle panel) summary bar graph showing effects on normalized mIPSC frequency, (lower panel) cumulative frequency curves for effects on inter-event interval. PSNCBAM-1 lacked effects on mIPSCs; AM251 significantly increased mean normalised mIPSC frequency (* $p < 0.01$ versus control (CTL), Student's *t*-test) and caused a significant leftward shift of the CTL inter-event interval curve ($p < 0.0001$ in individual cells, Kolmogorov-Smirnov test).

Figure 5. Effect of PSNCBAM-1 and AM251 on WIN55 actions

MOL #68197

A) Effect of 5 μ M WIN55 and subsequent application of 2 μ M AM251 (n=7) on mIPSCs; (upper panel) summary bar graph showing effects on normalized mIPSC frequency, (lower panel) cumulative frequency curves for effects on inter-event interval. WIN55 caused a reduction in normalised mIPSC frequency (* p <0.01, Student's t -test) which was reversed beyond control (CTL) levels by AM251 (** p <0.001, repeated measurement one-way ANOVA followed by a Tukey's HSD test). These data were reflected by significant shifts of the CTL inter-event interval curve for each treatment (both p <0.0001 in individual cells; Kolmogorov-Smirnov test). B) Effect of 5 μ M WIN55 and subsequent applications of 10 μ M PSNCBAM-1 and then 2 μ M AM251 (n=8) on mIPSCs; (upper panel) summary bar graph showing effects on normalized mIPSC frequency, (lower panel) cumulative frequency curves for effects on inter-event interval. WIN55 caused a reduction in normalised mIPSC frequency (* p <0.01, Student's t -test) which was not affected by PSNCBAM-1, but was increased by AM251 (* p <0.01, repeated measurement one-way ANOVA followed by a Tukey's HSD test). These data were reflected by significant shifts of the inter-event interval curve for WIN55 and AM251 treatment (both p <0.0001 in individual cells, Kolmogorov-Smirnov test), but a lack of effect of PSNCBAM-1.

Figure 6. Effect of PSNCBAM-1 on AM251

Effect of 2 μ M AM251 and subsequent application of 10 μ M PSNCBAM-1 (n=7) on mIPSCs; (upper panel) example raw data traces, (lower left panel) summary bar graph showing effects on normalized mIPSC frequency, (lower right panel) cumulative

MOL #68197

frequency curves for effects on inter-event interval. AM251 caused an increase in mean normalised mIPSC frequency (* $p < 0.01$, Student's t -test) which was reversed to control (CTL) levels by PSNCBAM-1 (* $p < 0.01$, repeated measurement one-way ANOVA followed by a Tukey's HSD test). These data were reflected by significant shifts of the inter-event interval curve for each treatment (both $p < 0.0001$ in individual cells, Kolmogorov-Smirnov test).

Figure 7. Effect of pre-treatment with PSNCBAM-1 on GABA_B-mediated inhibition at IN-PC synapses

Effect of 20 μ M baclofen on A) control mIPSCs (n=4) and B) in the presence of 10 μ M PSNCBAM-1 (n=5); (upper panel) example raw data traces, (lower panel) summary bar graph showing effects on normalized mIPSC frequency. PSNCBAM-1 had no effect on baclofen action, such that a baclofen-mediated significant reduction in normalised mIPSC frequency was seen under both conditions (* $p < 0.01$, Student's t -test).

Figure 1

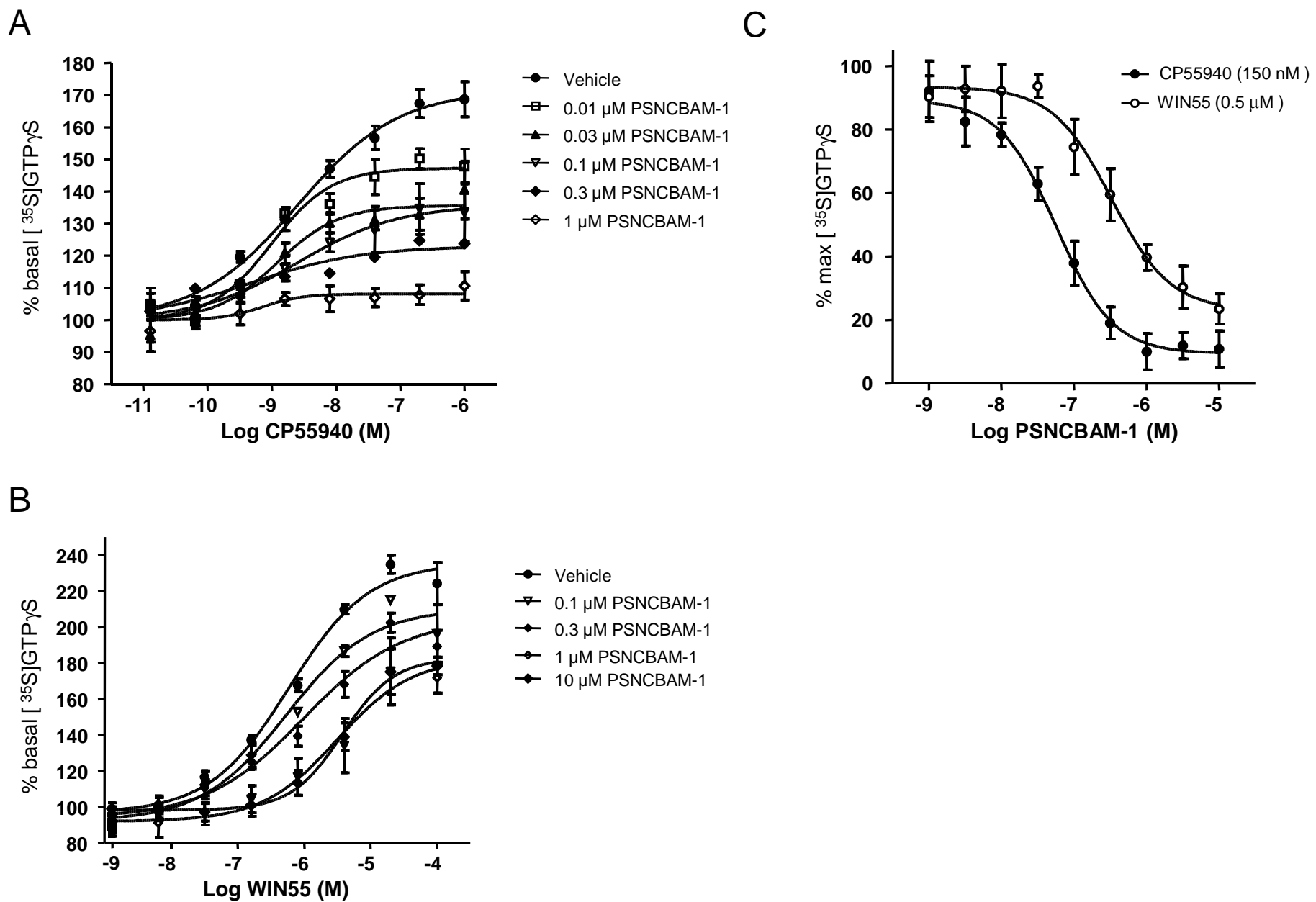


Figure 2

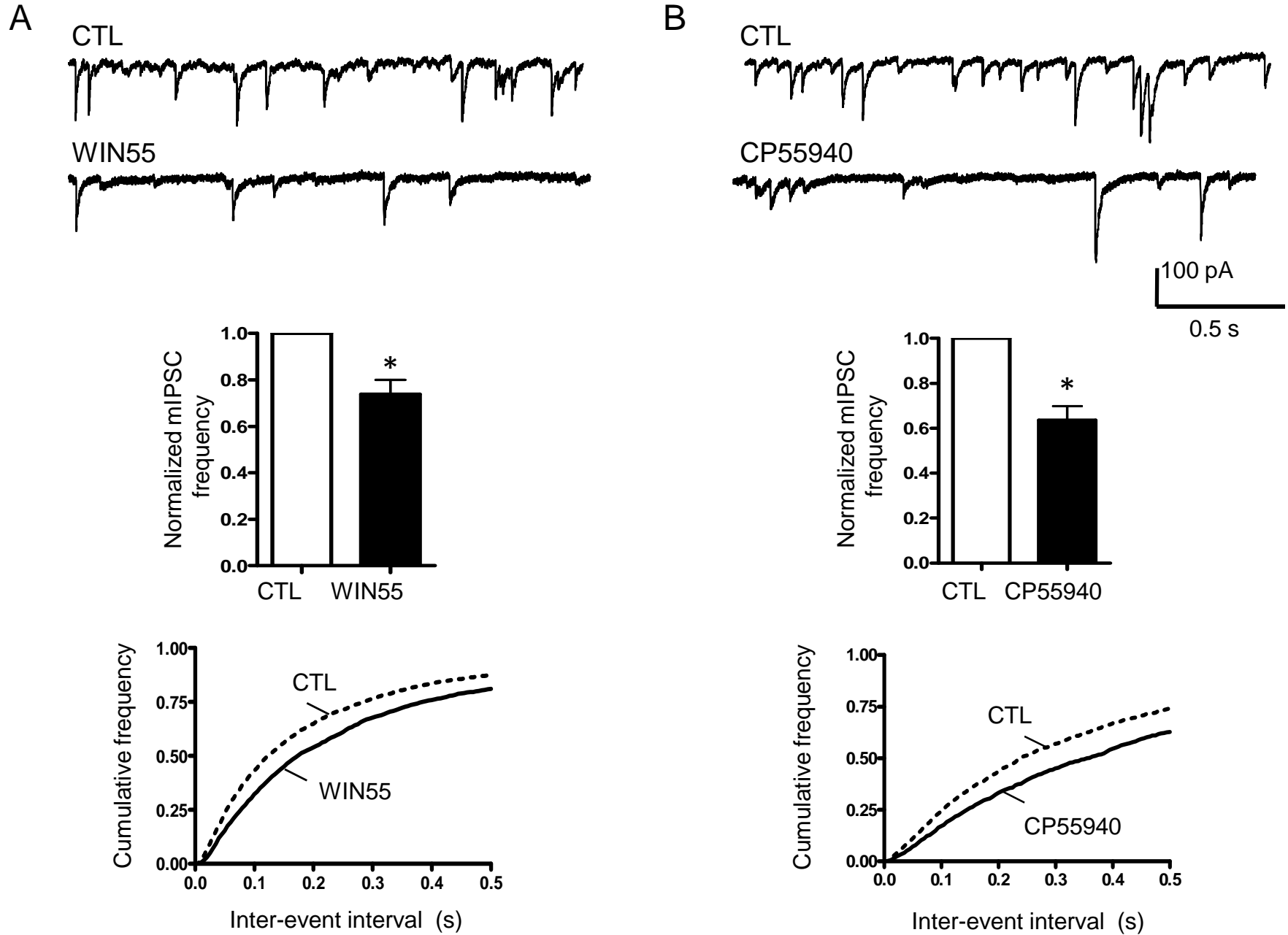


Figure 3

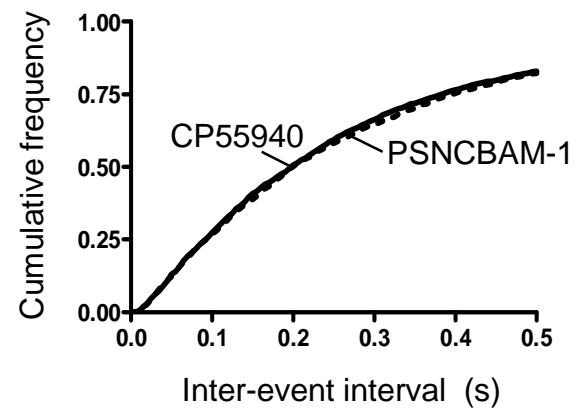
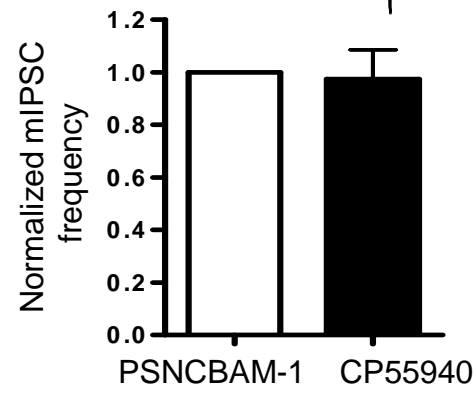
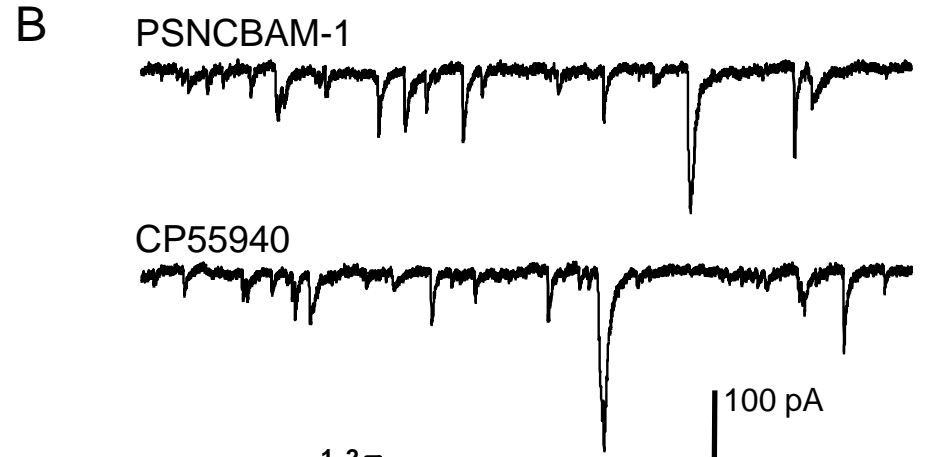
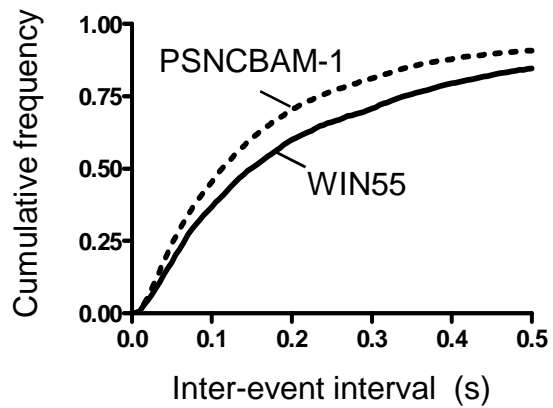
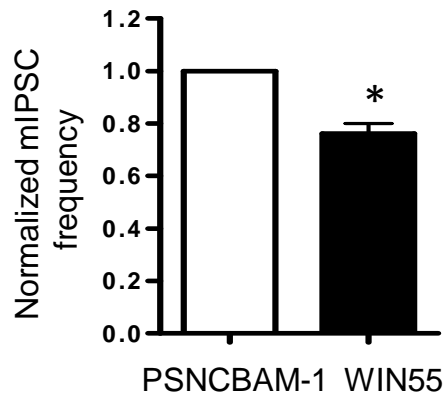
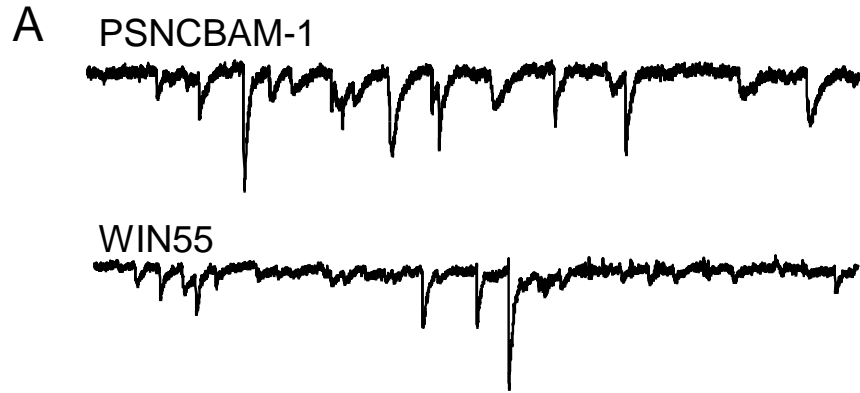


Figure 4

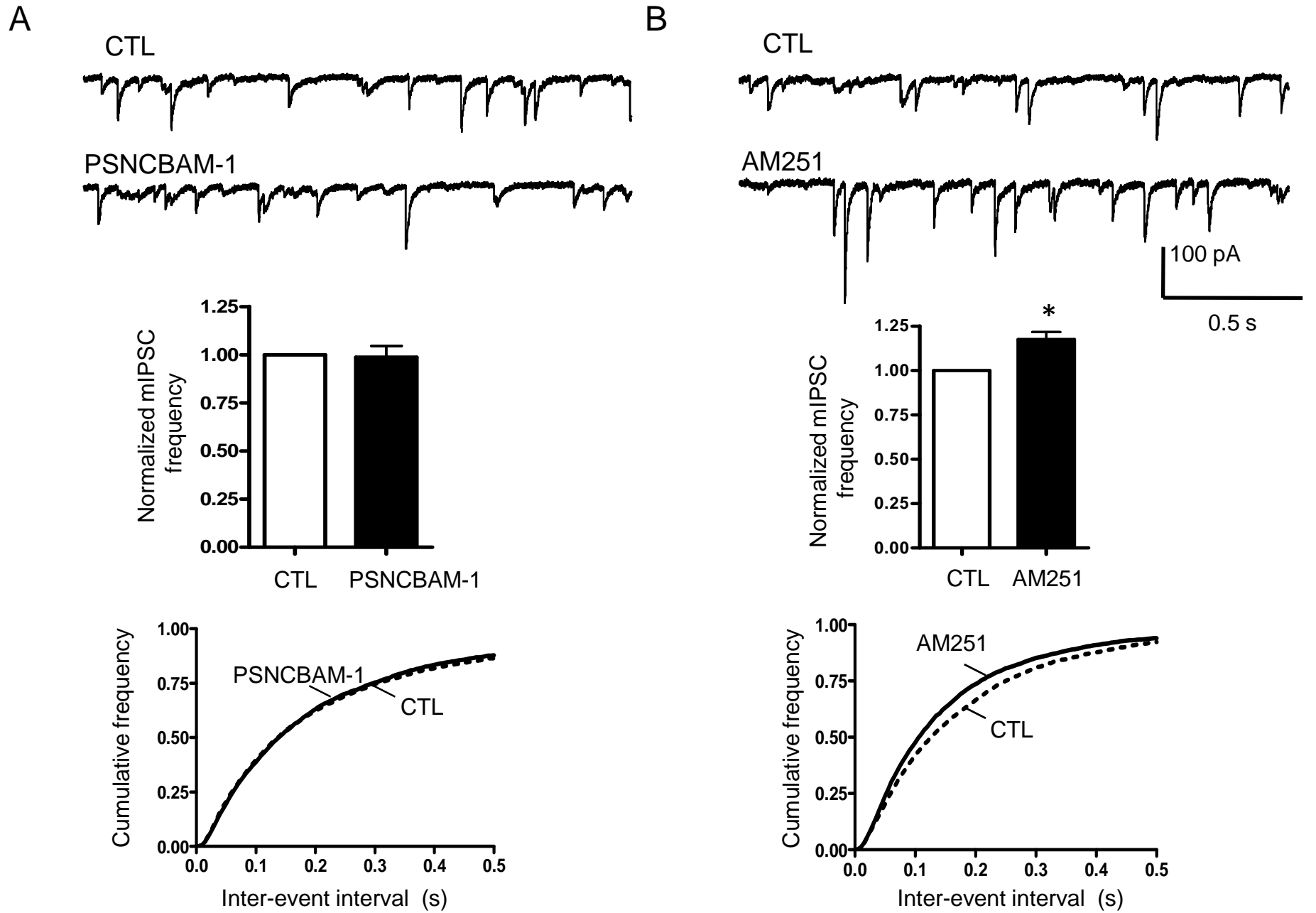
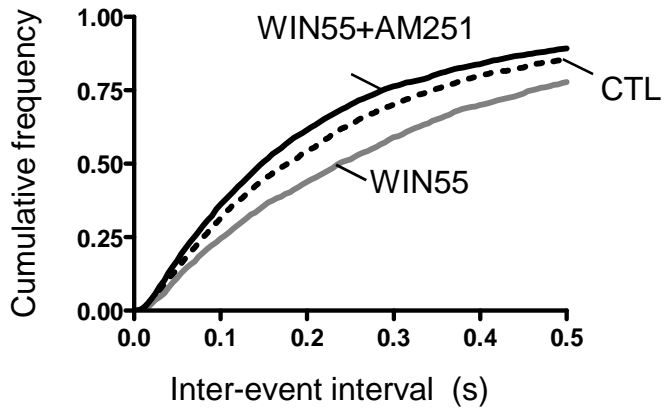
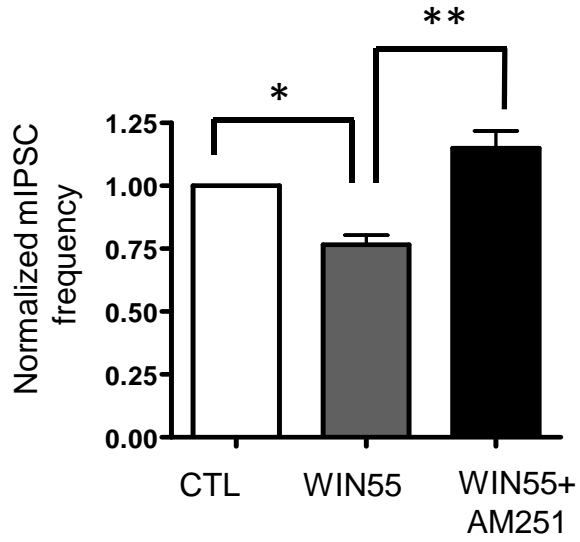


Figure 5

A



B

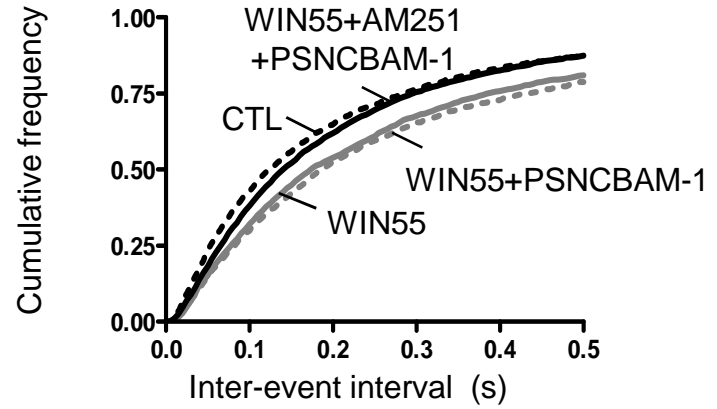
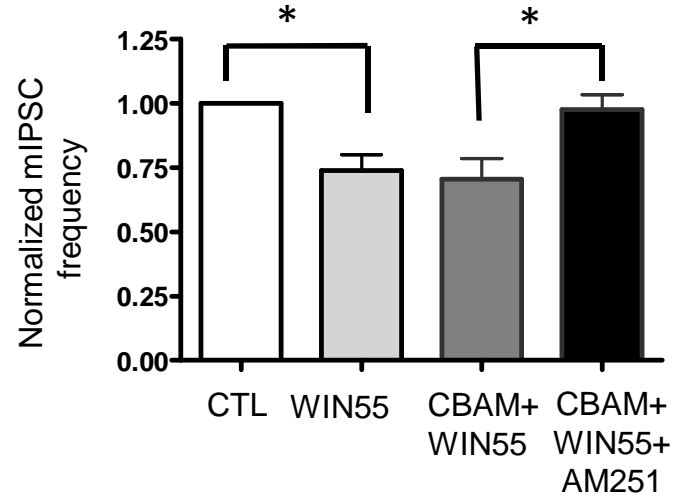


Figure 6

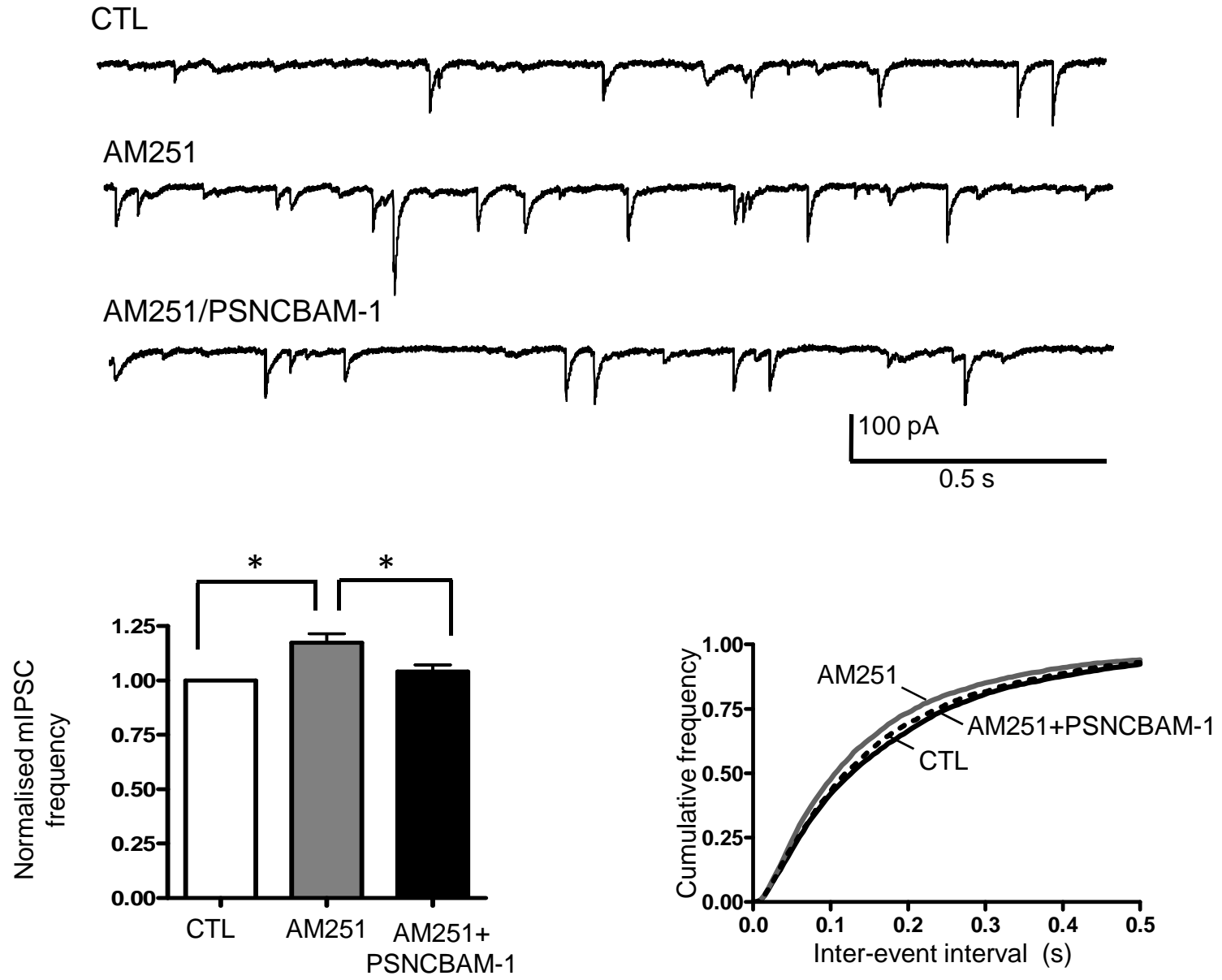
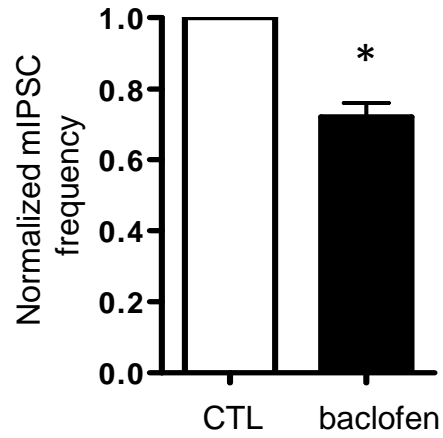
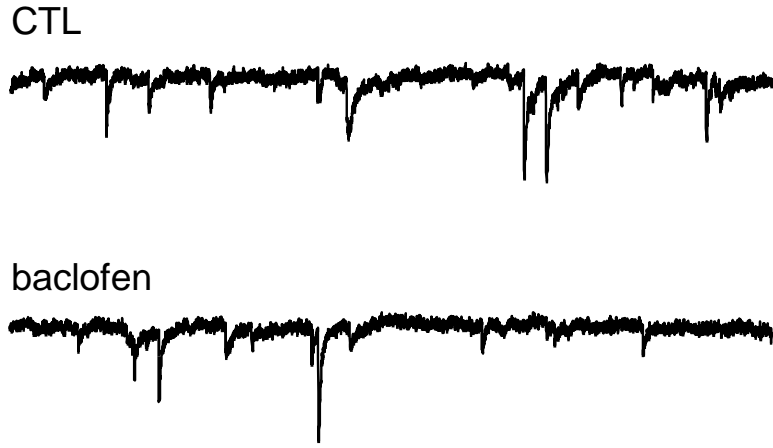


Figure 7

A



B

